Available online at www.sciencedirect.com
ScienceDirect
Journal of Hazardous Materials 143 (2007) 379–385
Journal of Hazardous Materials
www.elsevier.com/locate/jhazmat

Synthesis of ferrites obtained from heavy metal solutions using wet method

Ji Yang, Juan Peng, Kaicheng Liu, Rui Guo, Dianliang Xu, Jinping Jia *

School of Environmental Science and Engineering, Shanghai Jiao Tong University, Shanghai 200240, PR China

Received 24 April 2006; received in revised form 25 May 2006; accepted 14 September 2006
Available online 19 September 2006

Abstract

Wet method was employed to the treatment of heavy metal-contaminated wastewater, and $Zn_xFe_{3-x}O_4$, $Ni_xFe_{3-x}O_4$ and $Cr_xFe_{3-x}O_4$ ($0<x<1$) were synthesized. Phase identification of the prepared samples was done by X-ray diffraction (XRD), which indicates that the products are spinel-structured; transmission electron microscopy (TEM) images show that crystal size of the ferrite products synthesized is 0.1–0.4 μm. Thermostability of the products was characterized by differential thermal analysis (DTA) and thermal gravimetric analysis (TGA). It was found that when the doped ferrite is qualified, the highest content of doped ion (Zn^{2+}, Ni^{2+} and Cr^{3+}) that could enter ferrite lattice is: 0.08, 0.049 and 0.02, respectively. At low concentration the capability of doped ions entering ferrite product is $Ni^{2+} \approx Zn^{2+} > Cr^{3+}$ and the influence of the three ions on sample thermostability is $Zn^{2+} > Ni^{2+} > Cr^{3+}$.

Keywords: Ferrite; Heavy metal; Zinc; Nickel; Chrome; Stabilization

1. Introduction

With the wide use of heavy metals in industrial manufacturing operations, the treatment of wastewater contaminated by heavy metals, especially mining and electroplating wastewater becomes a serious environmental issue. In the cadmium (Cd) polluted Jinzu River basin in Toyama Prefecture, Japan, itai–itai disease prevailed in middle 1900s, which could cause bone brittleness and kidney failures and was officially recognized in 1968 as the first disease induced by environmental pollution in Japan after legal proceedings. Excessive exposure to heavy metals or overdrinking of water containing excessive heavy metals may cause toxicosis or even cancer to human beings. Take chromium for example, some of hexavalent chromium compound are viewed as strong oxidants and irritant poisons to mucosal tissues. Poisoning effects of these compounds may include metabolic acidosis, acute tubular necrosis, kidney failure and death [1].

Chemical precipitation method is usually used for the treatment of water polluted by heavy metals. But heavy metals cannot be degraded or destroyed; even though they can be efficiently removed from water, heavy metal sludge generated still will release harmful heavy metals to soil and groundwater when it is landfilled. Many methods were developed to stabilize the heavy metals, including solidifying and stabilizing by fixing the heavy metal sludge in cementitious solid products [2] or in the leach-resistant solid bodies [3]. Electrolytic ferrite method [4] and biological methods [5,6] were also employed. But the possible secondary pollution these methods may cause is still disputable, not to speak of the heavy cost.

The proposal of "ferrite process" carves out a new way for mining and electroplating wastewater/sludge disposal and utilization. In wet method of "ferrite process", the heavy metal ions are incorporated into the lattice points of ferrites during the formation of spinel structure by the oxidation of the Fe(II) ions [7] and these doped ferrites could still be used as environment-friendly magnetic materials or ferrite pigments with no harm. Many investigations have been developed on the formation of ferrites containing Al, Cr, Cu, Mg, Mn, Ni, Zn, etc., and physical and chemical properties of these ferrite composites

* Corresponding author. Tel.: +86 21 54742817; fax: +86 21 54742817.
E-mail address: yangji@sjtu.edu.cn (J. Jia).

0304-3894/$ – see front matter © 2006 Elsevier B.V. All rights reserved.
doi:10.1016/j.jhazmat.2006.09.038

have been studied as well [8–11]. Application of ferrite process have been employed in wastewater treatment [11], acid mine drainage treatment [12], municipal solid waste incineration ash treatment [13], etc. It will be greatly meaningful to apply low-cost wet method to heavy metal-contaminated water treatment.

However, the relationship between heavy metal ions and the quality of ferrites still needs further investigation. Also, as an important index in ferrite application, thermostability of synthesized ferrite products have seldom been deeply investigated. In this paper, three popular heavy metal ions in wastewater, Zn(II), Ni(II), Cr(III), were chosen to study the synthesis of doped ferrites. Ferrite products containing heavy metal ions with different concentrations were characterized and compared. Last but not least, differential thermal analysis and thermal gravimetric analysis were introduced in product characterization to test their thermostability, which could be used for reference in further investigation and application.

2. Materials and methods

2.1. Preparation of Fe/Zn, Fe/Cr and Fe/Ni-substituted ferrite

All the reagents used in the synthesis of doped ferrite were of analytical grade and were purchased from Sinopharm Group Chemical Reagent Co., Ltd. of China.

Doped ferrites were prepared as follows: standard solution of Zn, Ni, or Cr (prepared with deionized water and $ZnSO_4{\cdot}7H_2O$, $NiSO_4{\cdot}6H_2O$ or $Cr_2(SO_4)_3{\cdot}6H_2O$, respectively.) was mixed with standard solution of Fe (prepared with deionized water and $FeSO_4{\cdot}7H_2O$) with certain molar ratio in the reactor under the protection of nitrogen. The reactor was sealed with rubber septa and was kept in a thermostatic bath. Both of the solution was prepared with distilled water, of which dissolved oxygen and carbon dioxide were removed in advance. Then pH and volume of mixed solution was adjusted to a proper value for reaction. Optimum reaction condition was attained through orthogonal test.

A weak oxidant NH_4NO_3 was selected. Preliminary study showed that the amount of NH_4NO_3 influences the distribution of iron in different species greatly. $Fe(OH)_2$ is the main product with a low oxidant concentration. As the oxidant amount increases, the amount of $Fe(OH)_2$ decreases sharply and trivalent species increase. Fe_3O_4 become the main product when NH_4NO_3 reaches certain amount, while as the amount of oxidant goes on to increase, the amount of α-FeOOH increases greatly with a corresponding decrease in the amount of Fe_3O_4 and other by-products. From the aspect of thermodynamics, it seems that the amount of oxidant should be controlled in certain range so that neither $Fe(OH)_2$ nor α-FeOOH would become the main component of the product.

The reaction was carried on under the oxidation of 10 g/L NH_4NO_3 at 90 °C for 2 h. pH of the solution should be controlled between 9.0 and 11.0. Then the reaction solution was kept still for 2 h under constant temperature. The deposition of the solution was washed with deionized water for five times and acetone for three times. The sample acquired was dried under 60 °C and sealed in bottles for characterization.

2.2. Sample analysis

Content of doped ions was analyzed by X-ray fluorescence spectrometer with 20 kV, 20 mA, LiF(2 0 0) (Model VF-320, Shimadzu Co., Japan).

Transmission electron microscope (Model JEM-100CX, JEOL, Japan), Electrooptics analytical balance (Model TG328A, Shanghai Balance Instrument Factory, P.R. China), X-ray diffractometer (Model XD-3A, Shimadzu Co., Japan; Cu Kα radiation ($\lambda = 1.5418$ Å), 25 mA, 35 kV) with 4° min^{-1}, Electrooptics analytical balance (Model TG328A, Shanghai Balance Instrument Factory, P.R. China) were employed to characterize the samples.

Thermal analysis were performed by differential thermal analysis (Model CRY-1, Shanghai Balance Instrument Factory, P.R. China) from room temperature to 500 °C in air with a heating rate of 10 °C/min under a crosshead speed of 2 mm/min and thermal gravimetric analysis (Model PRT-1, Beijing Optical Instrument Factory, P.R. China) with a calefactive rate of 10 °C/min at a crosshead speed of 4 mm/min.

3. Results and discussion

3.1. Properties of doped ferrites containing Zn, Ni, or Cr element

As the concentration of doped ions increases to certain amount, deposition property of the solution became unsatisfying, and then tests of each group could end. Thus, the Zn group contains nine tests, and six tests in Ni group, five tests in Cr group.

By comparing amounts of doped ions and iron ions before reaction and in ferrite products, it was found that not all the metal ions entered lattice. However, the doped ions could barely be detected (always below 1 mg/L under the situations tested), which we assume that they might be trapped in the compound and co-precipitate. For better understanding of the results, content comparison instead of removal efficiency comparison was selected to indicate the ability and efficiency of doped ions entering lattice.

Table 1 shows the results of Zn group, Ni group and Cr group. It is conspicuous by comparing the content of doped-metal element and iron in doped ferrites of Table 1 that as the concentration of doped ions increases, the amount of corresponding element contained in doped ferrites increases as well. It could also be inferred that in a low concentration ($[Me]/([Me]+[Fe^{2+}]) = 0.02$), almost all the doped ions have entered spinel structure of ferrite products. But as the concentration increases, doped ion content in ferrite products changes as heavy metal element differs.

For Zn and Ni group, when the initial molar ratios is under 0.075, little difference could be told between the content of doped element before reaction and in product; while the amount

Table 1
Comparison of test results of Zn-, Ni- and Cr-doped ferrite

Label	Content of Me before reaction ($[Me^{n+}]^a/([Me^{n+}]+[Fe^{2+}])$)	Content of Me in doped ferrite ($[Me]/([Me]+[Fe_{total}])$)			Content of Fe in doped ferrite ($[Fe(II)]/([Me]+[Fe_{total}])$)		
		Zn	Ni	Cr	Zn	Ni	Cr
0	0	0	0	0	0.320	0.320	0.320
1	0.02	0.020	0.020	0.020	0.265	0.255	0.283
2	0.05	0.049	0.049	0.043	0.234	0.243	0.255
3	0.075	0.067	0.068	0.063	0.233	0.211	0.240
4	0.10	0.080	0.086	0.090	0.245	0.203	0.230
5	0.15	0.122	–[b]	–	0.143	–	–
6	0.20	0.135	0.168	–	0.154	0.171	–
7	0.22	0.161	–	–	0.098	–	–
8	0.25	0.200	–	–	0.073	–	–
9	0.30	0.257	0.221	–	0.021	0.122	–

[a] Me represents Zn, Ni or Cr. For Zn and Ni, $n=2$; for Cr, $n=3$.
[b] No test was carried on in the corresponding group.

of Cr entering ferrite structure is relatively fewer. It implies that at a lower concentration the capability sequence of doped ions entering ferrite product is: Ni ≈ Zn > Cr.

As the ratio rises from 0.075 to 0.10, Cr element enters into ferrite the most instead. But the products are not qualified as ferrites. With a concentration ratio under 0.3, Ni content in doped ferrite is a little more than that of Zn element. It was found that when the doped ferrite is qualified, the highest content of doped ion (Zn^{2+}, Ni^{2+} and Cr^{3+}) that could enter ferrite lattice is: 0.08, 0.049 and 0.02, respectively.

Researches showed that the incorporation of metal ions into the lattice points is mostly related to their ionic radii [14,15]. By comparing the content of the three metals in doped ferrites, it could be deduced that the capability of heavy metal ions entering ferrite structure might have some relationship with the solubility product constants of their corresponding hydroxides (Eqs. (1)–(3)) [16], and heavy metal ion with a relatively high hydroxides solubility product constant might enter spinel lattice easier:

$$K_{sp}[Ni(OH)_2] = 2.0 \times 10^{-15} \quad (1)$$

$$K_{sp}[Zn(OH)_2] = 1.2 \times 10^{-17} \quad (2)$$

$$K_{sp}[Cr(OH)_3] = 6.3 \times 10^{-31} \quad (3)$$

3.2. X-ray diffraction results and lattice constant comparison

X-ray diffraction results showed that all the iron black products are of spinel structure, which testified that they are all ferrites and that doped ions have assuredly entered the spinel structure. Fig. 1 shows a typical X-ray diffraction curve of Cr-doped ferrite [17]. Lattice constant values of products were obtained by analyzing corresponding X-ray diffraction results using a least-squares method [18].

Lattice constants are the lengths of the edges of a unit cell along its major axes. The smallest regularly repeated volume in a lattice is called a unit cell. Lattice constant values and knowledge of crystal structure are needed to calculate distances between neighboring atoms in a crystal, as well as in determining some of the crystal's important physical and electrical properties [19].

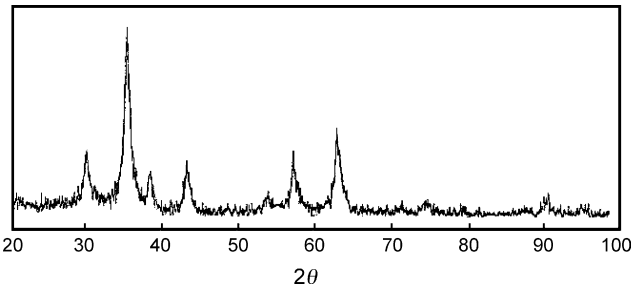

Fig. 1. X-ray diffraction curve of Cr-doped ferrite.

Also, lattice constant is a measure of structural compatibility between different materials.

Fig. 2 and Table 2 show the relationship between lattice constants and the content of doped metal elements in doped ferrite products.

Chemical composition of ferrite was expressed by the chemometric number (the value of x, which was obtained by tripling the content of each metal in doped ferrite) of doped metal element in ferrite product $Me_xFe_{3-x}O_4$ (Me represents Zn, Ni or Cr). Broken lines in Fig. 2 is ideal lines connecting lattice constant of Fe_3O_4 and $Me_xFe_{3-x}O_4$, which show that when Fe in ferrite is gradually replaced by heavy metal elements, lattice constant of the product changes linearly with the increase of x.

With the increase of x, lattice constant of Fe/Zn-substituted ferrite increases gradually (Fig. 2, curve of $Zn_xFe_{3-x}O_4$, except for the fourth sample), while lattice constant of Fe/Ni-substituted ferrite increases firstly and then decreases (Fig. 2, curve of $Zn_xFe_{3-x}O_4$). Relationship between Cr content and lattice constant of Cr-doped ferrite is irregular (Table 2).

Table 2
Relationship between Cr content and lattice constant of ferrite

	Label			
	1	2	3	4
$[Cr]/[Cr]+[Fe_{total}]$ in product	0.020	0.043	0.063	0.090
Lattice constant (Å)	8.413	8.416	8.397	8.414

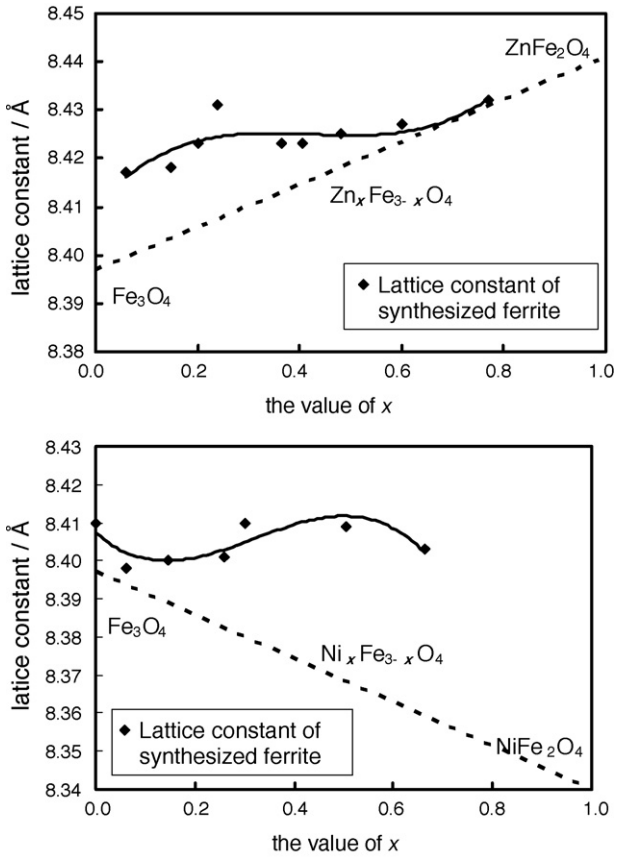

Fig. 2. Relationship between x and lattice constant of ferrite.

Fe_3O_4 crystal has an inverse spinel structure with a structural formula: $[Fe^{3+}]A[Fe^{3+}, Fe^{2+}]BO_4$. 'A' represents tetrahedral site where Fe ion is surrounded by four oxygen atoms, while 'B' represents octahedral site where Fe ion is surrounded by six oxygen atoms (Fig. 3).

Zn^{2+} ions tend to occupy the spinel on A-site [21], which force Fe^{3+} ions on A-site to enter B-site. But the ion radius of Zn^{2+} (0.82 Å) is larger than that of Fe^{3+} (0.67 Å), the four oxygen atoms constituting 'A' tetrahedral site have to move outward along the diagonal of lattice to provide more space for Zn^{2+} ion. Thus, lattice constant of doped ferrite appears to increase. As to the fourth sample of Zn group, the total content of Zn^{2+} ion and Fe^{2+} ion is the highest, which means the content of Fe^{3+} ion is

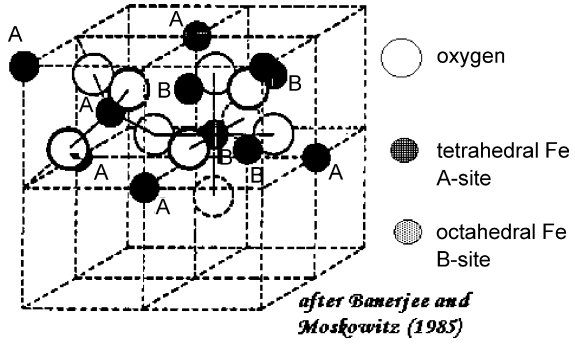

Fig. 3. The spinel structure of Fe_3O_4 crystal [20].

the least. Both the radius of Zn^{2+} ion and Fe^{2+} ion are larger than that of Fe^{3+} ion, so it is comprehensible that the lattice constant of sample 4 is a little higher.

Ni^{2+} ion and Cr^{3+} ion are B-site-entering ions, and the structure of Fe/Ni and Fe/Cr-substituted ferrite is quite different from that of Zn-doped ferrite. Fe^{2+} ion enters B-site easier than Fe^{3+} ion does, while Ni^{2+} ion and Cr^{3+} ion occupy B-site even more advantaged than Fe^{2+} ion does. When Ni^{2+} ions and Cr^{3+} ions go into ferrite lattice, they could not only replace Fe^{2+} ions on B-site, but also possibly push part of the Fe^{3+} ions into A-site and cause an increase in lattice constant. But with the increasing content of Ni^{2+} ions, lattice constant of Fe/Ni-substituted ferrite will decrease instead, due to Ni^{2+} ion's smaller radius (0.78 Å) comparing to Fe^{2+} ion (0.83 Å).

As for Cr^{3+} ion, it seems that it can only replace Fe^{3+} ion on B-site, but in fact, it can replace both Fe^{3+} ion and Fe^{2+} ion equally [22]. And Fe^{3+} ion and Fe^{2+} ion can also transform to each other through charge transfer. So the lattice constant change of Fe/Cr-substituted ferrite is the result of combining effects of Cr^{3+} ions, Fe^{3+} ions and Fe^{2+} ions. Robbins et al. [22] reported that when x value changes from 0 to 2, lattice constant of Cr-doped ferrite differs dramatically. The irregularity of lattice constant data in Table 2 coincides with their results.

3.3. Thermostability of doped ferrites

Fig. 4a–c illustrates the DTA curves of doped ferrites containing Zn^{2+}, Ni^{2+} and Cr^{3+}, respectively. In the curve of $Ni_xFe_{3-x}O_4$, while x is 0.504 and 0.663, small endothermic peak appears. While in the curve of $Cr_xFe_{3-x}O_4$, endothermic peak appears when x is only 0.129, and the peak becomes larger as the content of Cr increases; TG analysis shows that it is due to the dehydration of samples (Fig. 5). There is barely any endothermic peak in the curve of Zn-doped samples.

In Ni group, large and sharp peaks appear in samples 2–4 ($x = 0.147, 0.204, 0.258$). But the peak heights of the three samples reduce successively. In curves of samples 6 and 9 ($x = 0.504$, 0.663), the peaks become plain. The phenomenon of successive debasing of exothermic peak is caused by the gradual decrease of Fe content in samples, and it appears in Zn group as well. As for the formation of large and sharp peak, it may due to the fact that Fe^{2+} and Ni^{2+} ions do not enter the ferrite lattice synchronously during ferrite formation, which means that the crystal core consists of Fe_3O_4, and with the growth of the crystal, Ni^{2+} ions begin to be absorbed by the outer layer of the crystal and enter the lattice together with Fe^{3+} ions. Thus, the outer layer of the crystal is mainly constituted with $Ni_xFe_{3-x}O_4$, which is difficult to oxidize. As the thermostability of $Ni_xFe_{3-x}O_4$ is better than that of pure ferrite, when it comes to the oxidation temperature of $Ni_xFe_{3-x}O_4$, the inner part of the crystal get oxidized immediately and sharp peak appears.

Fig. 5 shows the TG analysis curves of several selected samples. A net weight loss appears the TG curve of sample 4 of Cr group, and it may caused by the low content of Fe^{2+} in the sample. It could be found by comparing TG and DTA curves that the second peak in DTA curve is oxidation exothermic peak

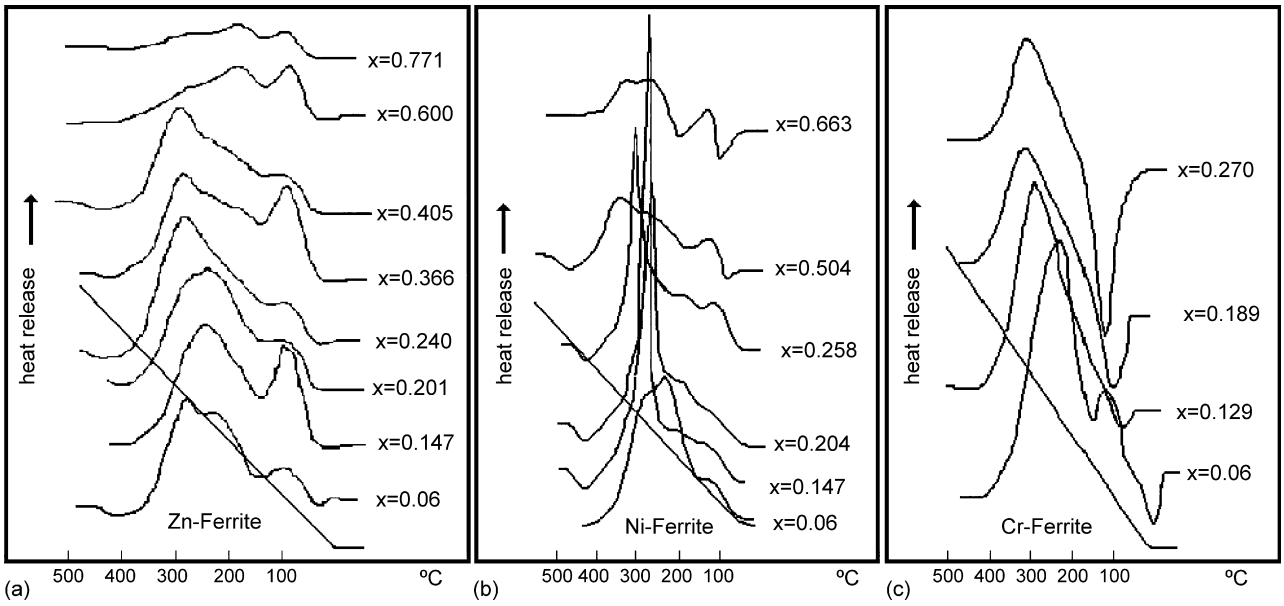

Fig. 4. DTA curve of doped ferrite containing Zn^{2+} (a), Ni^{2+} (b) and Cr^{3+} (c).

which represents the thermostability of ferrite samples. When the second peak appears, the sample begins to be oxidized and its weight increases. Thus, a relationship between oxidation temperature and doped ion content could be deduced though analyzing DTA curve of each samples, and it is illustrated in Fig. 6.

It is shown in Fig. 6 that thermostability of Cr-doped ferrite is quite different from that of Ni- and Zn-doped ferrite. With the content of doped ion increases, thermostability of Fe/Zn and Fe/Ni-substituted ferrite increases rapidly and then decreases rapidly before tending to plain, while thermostability of Fe/Cr-substituted ferrite increases continually, and at doped-ion content under 0.12, it increases most rapidly in the three groups. It seems that under an x value of 0.12, the content of Zn^{2+} ions influences sample thermostability most, while the content of Cr^{3+} ions influences least. When the x value is above 0.12, the sequence is just the opposite. It could be seen from the test results of the three groups that doped ion content is usually small if the doped ferrite is to be qualified. So the influence sequence is usually list as: $Zn^{2+} > Ni^{2+} > Cr^{3+}$.

3.4. Crystal size of samples

Fig. 7 illustrates crystal images of doped ferrites. The size of crystals is between 0.1 and 0.4 μm. Ferrites containing Zn are mostly spherical crystals with a few cubic particles, and ferrites containing high ratio of Zn become irregular-shaped (sample 9, $x = 0.771$). Fe/Cr-substituted ferrite crystals are mostly cubic, while Ni-doped ferrite crystals turn out to be both spherical and cubic. It could be seen from Fig. 7 that crystals become irregular as the content of doped metal ions increases, and Ni-doped ferrite crystals become irregular at a low content of Ni^{2+} ion content. It could be concluded that the influence sequence of the three metal ions on ferrite crystal shape is: $Ni^{2+} > Cr^{3+} > Zn^{2+}$.

And also it could be deduced by analyzing Fig. 4 and the size difference of TEM images of samples that it is more difficult

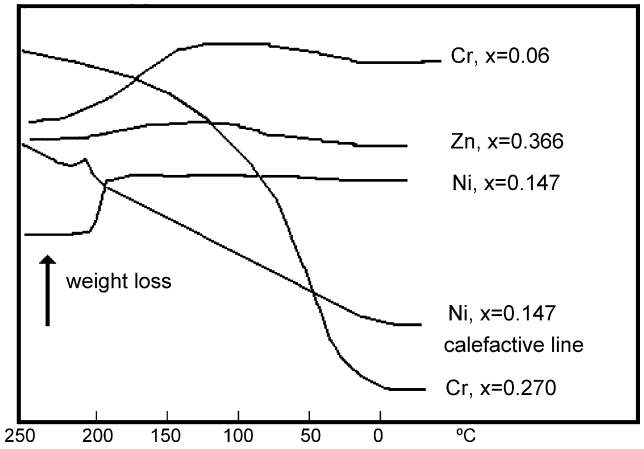

Fig. 5. TG curves of selected samples.

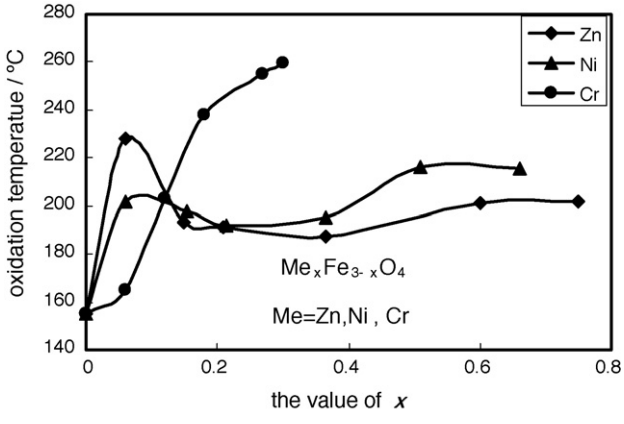

Fig. 6. Relationship between oxidation temperature and doped ion content.

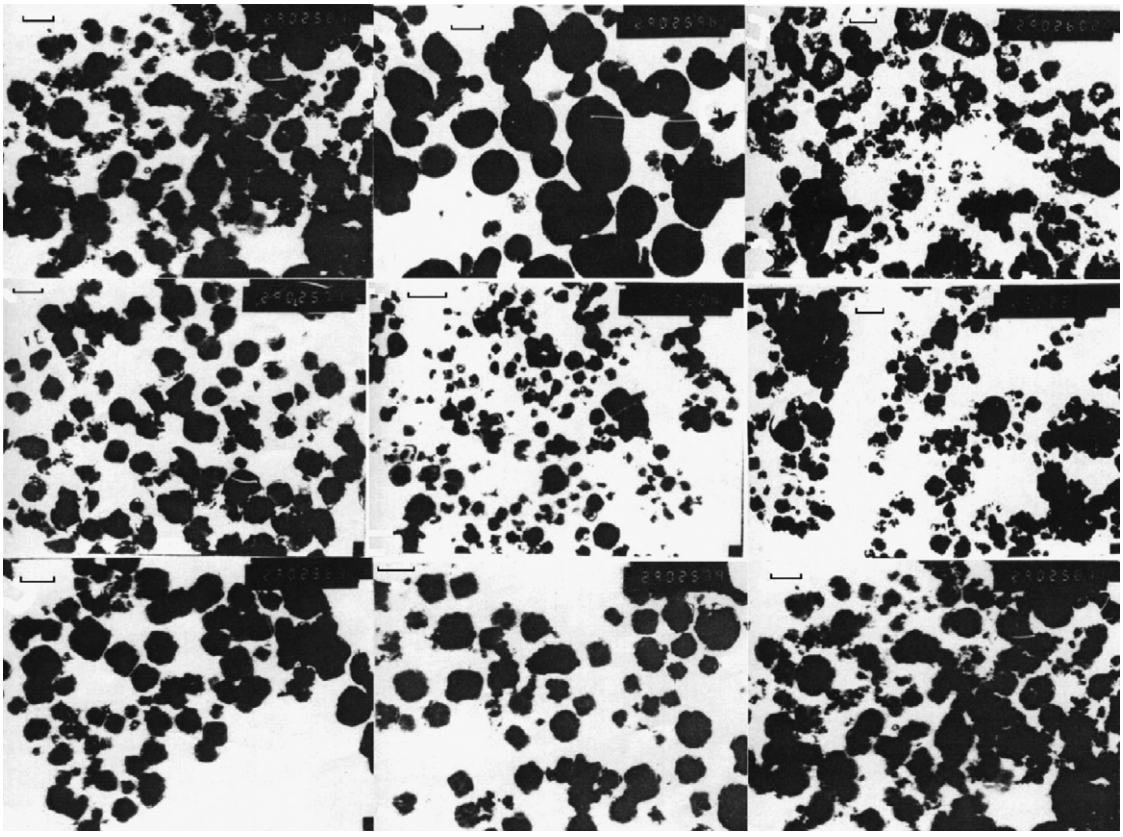

Fig. 7. TEM images of doped ferrites (row 1: $Zn_xFe_{3-x}O_4$, $x=0.06$, 0.405, 0.771, respectively; row 2: $Ni_xFe_{3-x}O_4$, $x=0.147$, 0.258, 0.663, respectively; row 3: $Cr_xFe_{3-x}O_4$, $x=0.06$, 0.129, 0.270, respectively. Scale in each image represents 0.3 μm).

to synthesize high-Ni/Cr-content anhydrous ferrite with larger crystal size than to synthesize counterpart Zn-doped ferrite.

4. Conclusions

1. At low concentration the capability of doped ions entering ferrite product is: $Ni^{2+} \approx Zn^{2+} > Cr^{3+}$. When the doped ferrite is qualified, the highest content of doped ion (Zn^{2+}, Ni^{2+} and Cr^{3+}) that could enter ferrite lattice is: 0.08, 0.049 and 0.02, respectively. Although ionic radius determines the capability of corresponding metal ions entering ferrite structure mostly, solubility product constants of their corresponding hydroxides also might have some relationship with it.
2. With the increase of x, lattice constants of Zn- and Ni-doped ferrite change regularly, while relationship between Cr content and lattice constant of Cr-doped-ferrite is irregular.
3. Thermostability of doped ferrite is better than that of pure ferrite. The influence sequence of the three ions on sample thermostability is $Zn^{2+} > Ni^{2+} > Cr^{3+}$ under the content ratio of 0.12. When Cr and Ni content are high, the crystals of doped ferrites become smaller and irregular, and more water is contained in ferrite products. Thus, in DTA curve, endothermic peak will appear, and weight loss will be obvious in TG curve.
4. Crystals of Zn-doped ferrite are mainly spherical and crystals of Cr-doped ferrite are mainly cubic. Crystals of Ni-doped ferrite appear both spherical and cubic. It seems difficult to synthesize highly doped and anhydrous Fe/Ni- or Fe/Cr-substituted ferrite with larger crystals through wet method.

Acknowledgements

This research is based upon work supported by the Natural Science Foundation of China (Project No. 20507014). Any opinions, findings, conclusions, or recommendations expressed in this publication are those of the authors and do not necessarily reflect the view of the supporting organizations. The authors are grateful to Yalin Wang for advice and troubleshooting the experimental apparatus and sample analysis.

References

[1] L.A. Saryan, M. Reedy, Chromium determinations in a case of chromic acid ingestion, J. Anal. Toxicol. 12 (1988) 162–164.
[2] K.S. Chen, H.W. Majewski, Disposal of heavy metal containing sludge wastes, US Patent 4,113,504 (1978).
[3] R.W. Styron, Leach-resistant solid bodies from fly ash and heavy metal sludge, US Patent 4,226,630 (1980).
[4] N. Nojiri, N. Tanaka, K. Sato, et al., Electrolytic ferrite formation system for heavy-metal removal, J. Water Pollut. Control Fed. 52 (1980) 1898–1906.
[5] B.W. Afkinson, et al., Bioremediation of metal contaminated industrial effluent using waste sludges, Water Sci. Technol. 34 (1996) 9–15.
[6] M. Gavrilescu, Removal of heavy metals from the environment by biosorption, Eng. Life Sci. 4 (2004) 219–232.
[7] Y. Tamaura, T. Katsura, S. Rojarayanont, et al., Ferrite process—heavy-metal ions treatment system, Water Sci. Technol. 23 (1991) 1893–1900.

[8] F. Prieto, E. Barrado, J. Medina, F.A. López-Gómez, Characterisation of zinc bearing-ferrites obtained as by-products of hydrochemical waste-water purification processes, J. Alloys Compd. 325 (2001) 269–275.
[9] E. Barrado, F. Prieto, J. Medina, F.A. López, Characterisation of solid residues obtained on removal of Cr from waste water, J. Alloys Compd. 335 (2002) 203–209.
[10] E. Barrado, F. Prieto, F.J. Garay, et al., Characterization of nickel-bearing ferrites obtained as by-products of hydrochemical wastewater purification processes, Electrochim. Acta 47 (2002) 1959–1965.
[11] B. Demirel, O. Yenigun, M. Bekbolet, Removal of Cu, Ni and Zn from wastewaters by the ferrite process, Environ. Technol. 20 (1999) 963–970.
[12] W. McKinnon, J.W. Choung, Z. Xu, et al., Magnetic seed in ambient temperature ferrite process applied to acid mine drainage treatment, Environ. Sci. Technol. 34 (2000) 2576–2581.
[13] S.H. Hu, Stabilization of heavy metals in municipal solid waste incineration ash using mixed ferrous/ferric sulfate solution, J. Hazard. Mater. 123 (1–3) (2005) 158–164.
[14] L. Vegard, The constitution of mixed crystals and the space occupied by atoms, Z. Phys. 5 (1921) 17–26.
[15] L. Pauling, The use of atomic radii in the discussion of interatomic distances and lattice constants of crystals, Acta Cryst. 10 (1957) 685–687.
[16] R.H. Petrucci, W.S. Harwood, F.G. Herring, General Chemistry: Principles and Modern Applications, 8th ed., Prentice-Hall, Upper Saddle River, NJ, 2001.
[17] J.P. Jia, J. Yang, Z.J. Chen, et al., Treatment conditions of sediment of ammonia soaked and Cr extracted electroplating sludge by ferrite method, Environ. Sci. 3 (1999) 49–52.
[18] J.B. Nelson, D.P. Riley, An experimental investigation of extrapolation methods in the derivation of accurate unit-cell dimensions of crystals, Proc. Phys. Soc. 57 (1945) 160–177.
[19] http://semiconfareast.com/lattice_constants.htm.
[20] S.K. Banerjee, B.M. Moskowitz, Ferrimagnetic properties of magnetite, in magnetite biomineralization and magnetoreception in organisms: a new magnetism, in: J.L. Kirschvink, et al. (Eds.), Magnetite Biomineralization and Magnetoreception in Organisms: A New Magnetism, Plenum Publishing Corporation, New York, NY, 1985, pp. 17–41.
[21] Z.G. Zhou, Ferrite Magnetic Materials, Science Press, Beijing, China, 1981.
[22] M. Robbins, G.K. Wertheim, R.C. Sherwood, D.N.E. Buchanan, Magnetic properties and site distributions in the system $FeCr_2O_4$–Fe_3O_4, J. Phys. Chem. Solids 32 (1971) 717–729.